

## Study on Positronium Bose-Einstein Condensation

Akira Ishida<sup>1\*</sup>, Kenji Shu<sup>1</sup>, Tomoyuki Murayoshi<sup>1</sup>, Xing Fan<sup>1</sup>, Toshio Namba<sup>1</sup>,  
Shoji Asai<sup>1</sup>, Kosuke Yoshioka<sup>2</sup>, Makoto Kuwata-Gonokami<sup>1</sup>, Nagayasu Oshima<sup>3</sup>,  
Brian E. O'Rourke<sup>3</sup>, and Ryoichi Suzuki<sup>3</sup>

<sup>1</sup>Department of Physics, Graduate School of Science, and International Center for Elementary Particle Physics (ICEPP), the University of Tokyo, 7-3-1 Hongo, Bunkyo-ku, Tokyo 113-0033, Japan

<sup>2</sup>Photon Science Center (PSC), Graduate School of Engineering, the University of Tokyo, 7-3-1 Hongo, Bunkyo-ku, Tokyo 113-8656, Japan

<sup>3</sup>National Institute of Advanced Industrial Science and Technology (AIST), 1-1-1 Umezono, Tsukuba, Ibaraki 305-8568, Japan

E-mail: [ishida@icepp.s.u-tokyo.ac.jp](mailto:ishida@icepp.s.u-tokyo.ac.jp)

(Received September 25, 2017)

Realization of the Bose-Einstein condensation (BEC) of positronium is a long-standing challenge of positron physics. Since the positron is the antimatter of the electron, the positronium is the antimatter of itself, and its gravity interaction is a sum of matter and antimatter components. In this sense, it can be used to study antimatter gravity. It can also be used as a source of a  $\gamma$ -ray laser. We have proposed a new method to realize a positronium BEC: a combination of thermalization in a cold silica target and laser cooling using 1S-2P transitions. We have started some basic studies based on our new idea. Here we report a preliminary result of our positronium thermalization measurement in cryogenic environment and development status of a new laser system for positronium cooling.

### 1. Introduction

Positronium (Ps) is a purely leptonic bound system of an electron and a positron which is an antimatter of an electron. It has two spin eigenstates: *ortho*-positronium (*o*-Ps) which is a spin triplet state and decays into 3  $\gamma$ -rays in a lifetime of 142 ns, and *para*-positronium (*p*-Ps) which is a spin singlet state and decays into 2  $\gamma$ -rays in a lifetime of 125 ps. Many precision tests of bound-state quantum electrodynamics (QED), e.g. hyperfine splitting [1,2], *o*-Ps and *p*-Ps lifetimes [3,4], 1S-2S spectroscopy [5], etc. have been performed using Ps since it is free from hadronic uncertainties. Furthermore, using its unique characteristic of matter-antimatter system, it can be used to search for matter-antimatter asymmetries: e.g. searches for charge-parity (CP) or charge-parity-time (CPT) violations [6,7], and gravity measurement using 1S-2S precision spectroscopy [8] or an atomic interferometer [9].

The Bose-Einstein condensation of Ps (Ps-BEC) is one of the long-standing targets of positron and positronium physics. If realized it would be the first BEC of any system which contains an antiparticle. It has a strong potential for gravity measurement of antimatter since the positron is the antimatter of the electron and the Ps is the antimatter of itself, which means that the gravity interaction of the Ps is a sum of matter and antimatter components. It can also be used as a source of a  $\gamma$ -ray laser, which is expected to be a next-generation laser useful for high resolution medical imaging/surgery, precision non-destructive inspections, super-long-distance communications, etc. [10] The  $\gamma$ -ray laser can be realized by self-amplification of *p*-Ps annihilations, which are made by stimulated transitions from *o*-Ps BEC caused by irradiations of 203 GHz microwaves [11, 12]. The challenge is to form dense and cold Ps in a short lifetime of 142 ns. Figure 1 shows the relationship between density and BEC critical temperature for several kinds of atoms. Our goal to realize Ps-BEC is 14 K at  $10^{18} \text{ cm}^{-3}$ .

The critical temperature of Ps-BEC is much higher than that of other kinds of atoms since Ps is quite light (Ps mass is  $\sim 1/1000$  of hydrogen mass). However, the difficulties are to prepare such dense antiparticles and cool Ps down efficiently in a very short lifetime of 142 ns.

To overcome these difficulties, we propose the following method for realizing Ps-BEC [13, 14]. The method and a basic idea to focus positrons are summarized in Sec. 2. Preliminary results of Ps thermalization measurement in cryogenic environment are shown in Sec. 3. Status of the laser development is described in Sec. 4.

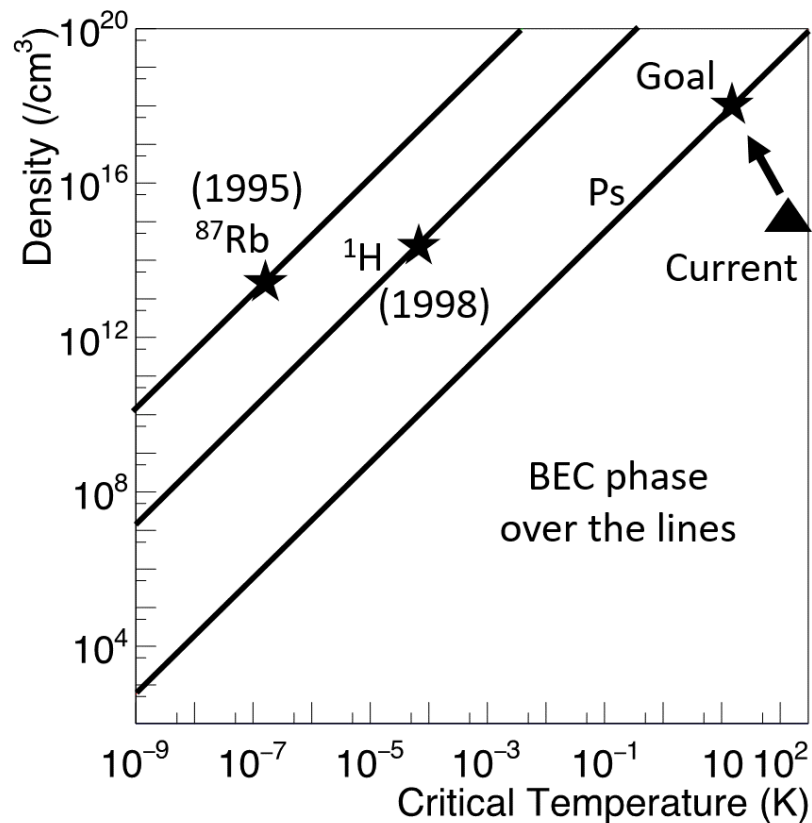


**Fig. 1** Relationship between density and BEC critical temperature for  $^{87}\text{Rb}$ ,  $^1\text{H}$ , and Ps atoms. The top-left region of each line shows the BEC phase for the corresponding atoms. The black triangle shows the current state-of-the-art Ps density, and the goal to realize Ps-BEC is shown by the star.

## 2. New method to realize Ps-BEC

### 2.1 Overall idea

Figure 2 shows a schematic view of our overall idea to realize Ps-BEC. To prepare dense Ps atoms, dense positrons are first created and then they are converted into dense Ps. A positron accumulator is used as the positron source. The positrons from the accumulator are ejected as a bunch of  $10^7$  positrons with keV energy. The positron bunch is focused to 100 nm beam waist and injected into a silica target which works as a Ps converter with as high as 50 % conversion fraction. Converted Ps are trapped in internal voids typical size of  $\sim 100 \text{ nm} \times 100 \text{ nm} \times 100 \text{ nm}$ , in each of which 4000 ps

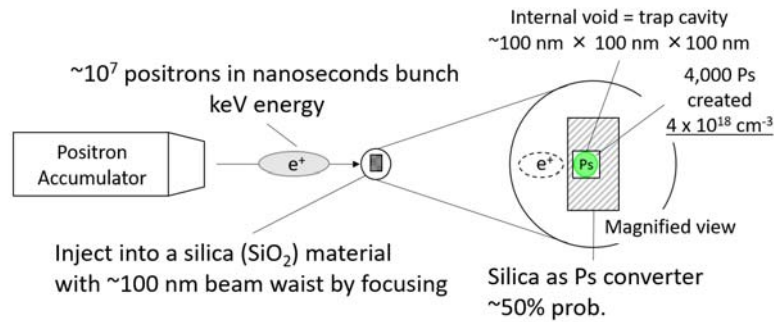


Fig. 2 Schematic view of our new method to realize Ps-BEC.

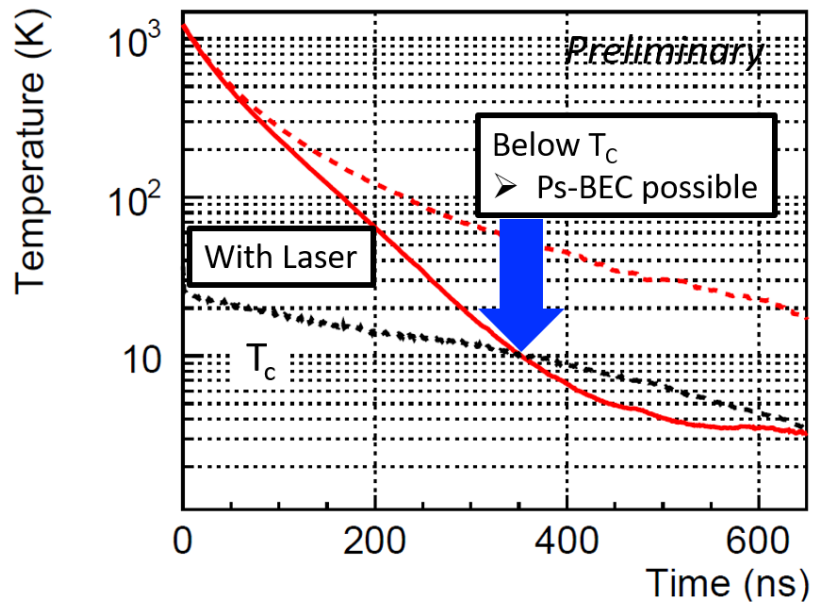
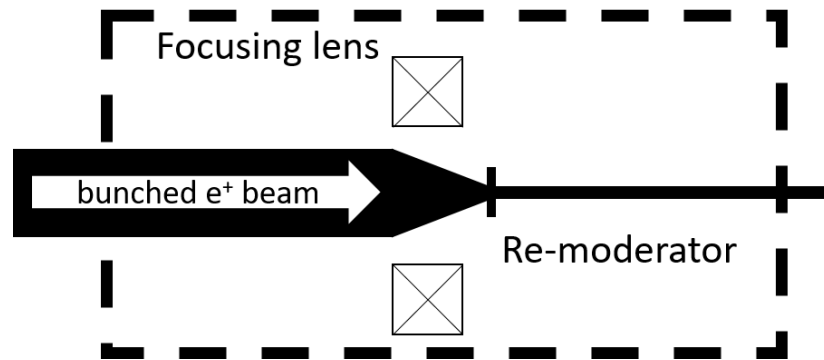


Fig. 3 Monte Carlo simulation of time evolution of Ps temperature. The solid line is with laser cooling, and upper dashed line is without laser cooling. The lower dashed line is the critical temperature of Ps-BEC.

( $4 \times 10^{18} \text{ cm}^{-3}$ ) are created at first.

Converted Ps has ~1 eV kinetic energy. To prepare cold Ps atoms, two-stage cooling is used. The first stage is Ps thermalization where Ps are cooled by momentum transfer to the cold silica cavity with collisions. The second stage is Ps laser Doppler cooling using 1S-2P transitions. Figure 3 shows a Monte Carlo simulation of the time evolution of Ps temperature. The preliminary results of our Ps thermalization parameters (Sec. 3) are used. The laser parameters are summarized in Sec. 4. The Ps thermalization quickly cools Ps down to ~300 K, but it is not enough to realize Ps-BEC. Below ~300 K, the Ps laser cooling effect is dominant and it cools Ps sufficiently. The simulation shows that a Ps-BEC can be realized at around 350 ns after Ps formation using our new method.



**Fig. 4** The basic idea of positron focusing. The brightness enhancement system is used for multiple stages.

### 2.2 Positron focusing

Figure 4 shows the basic idea of positron focusing to 100 nm waist. In principle, a positron brightness enhancement system using a focusing lens and a remoderator can be used [15]. By using this system, parallel and monoenergetic positron beams can be obtained. To focus an order of magnitude stronger than the current state-of-the-art  $\mu\text{m}$  waist beams, the brightness enhancement system will be repeated for multiple stages.

Possible problems to be solved are the following: space charge of the beam, discharge, charging up, and heating up of the Ps conversion target. It is important to measure the beam-density dependence of the brightness enhancement efficiency, the charging up effect of the target, and the temperature of the target using bunched positron beams.

## 3. Measurement of Ps thermalization process in cryogenic environment

### 3.1 Motivation

The Ps thermalization process is used as the first-stage cooling to realize a Ps-BEC in our new idea. Time evolution of the Ps kinetic energy by thermalization in a silica target is described by the following equation [16].

$$\frac{dE}{dt} = -\frac{2}{LM}v \left( E - \frac{3}{2}k_B T \right), \quad (1)$$

where  $E$  is the Ps kinetic energy,  $t$  is time since Ps formation,  $L$  is Ps mean free path,  $M$  is an effective mass of silica for elastic collision with Ps,  $v = \sqrt{2E/m_{\text{Ps}}}$  is Ps velocity,  $m_{\text{Ps}}$  is Ps mass,  $k_B$  is the Boltzmann constant, and  $T$  is the temperature of the silica target. The important parameter is  $M$ ,

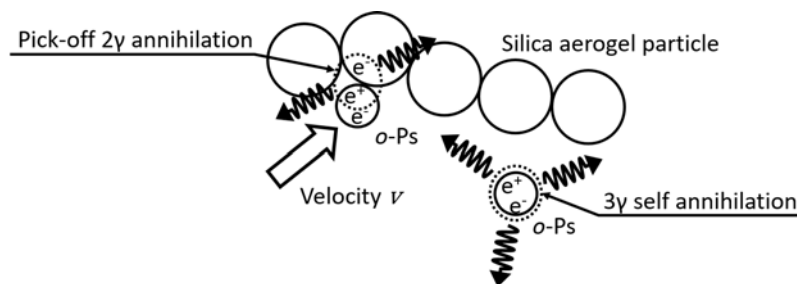


**Fig. 5** Two different annihilations of *o*-Ps in a silica aerogel target.

which essentially determines how quickly Ps are thermalized. There are several measurements of  $M$  [16–19] as summarized in Ref. 11, but they are all at higher temperature than 300 K, and the uncertainty of the measurements is so large that it is difficult to optimize the geometry of the silica target and laser specifications. An alternative, precise measurement of the Ps thermalization process in a cryogenic environment is necessary to solve these problems.

### 3.2 Method

The pick-off annihilation of  $o$ -Ps is used for the measurement. Figure 5 shows two different annihilations of  $o$ -Ps in a silica target. The  $3\gamma$  self annihilation is the same annihilation as in vacuum. A positron of a Ps atom annihilates with an electron in the same Ps atom. The decay  $\gamma$ -rays make a continuous energy spectrum from zero to 511 keV. On the other hand, the pick-off  $2\gamma$  annihilation does not occur in vacuum, but it only occurs by collisions with the surrounding material. It is an annihilation of a positron in a Ps atom with an electron in the silica target. The decay  $\gamma$ -rays have a monochromatic energy spectrum at 511 keV.

The pick-off annihilation rate  $\lambda_2$  can be naively assumed to be proportional to  $n\sigma v$ , where  $n$  is density of electrons in the silica particle, and  $\sigma$  is the cross section of the pick-off annihilation. Under this assumption, the time evolution of Ps velocity  $v$  can be measured by measuring  $\lambda_2$  as a function of Ps lifetime.

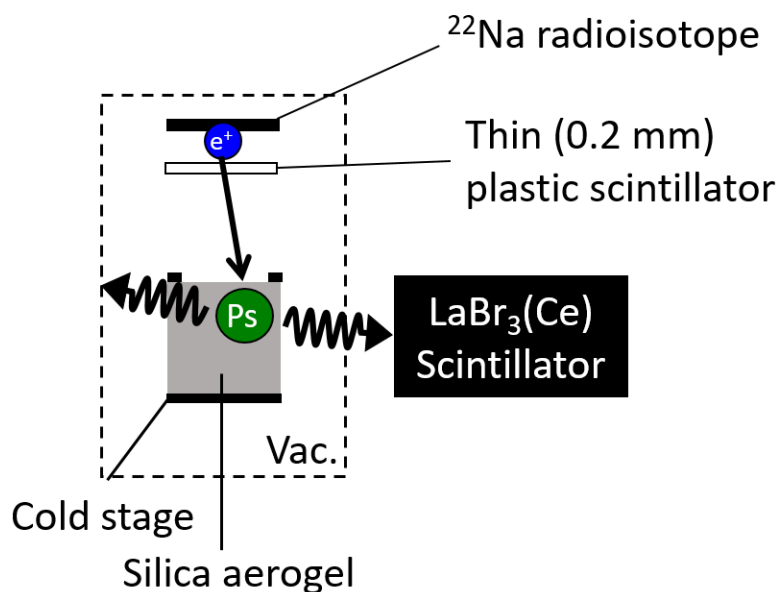


**Fig. 6** Schematic view of the experimental setup of the Ps thermalization measurement.

### 3.3 Experimental setup

Figure 6 shows a schematic diagram of the experimental setup and Fig. 7 shows photographs of the setup. The entire system except for the  $\text{LaBr}_3(\text{Ce})$  scintillator and two fine-mesh PMTs are located inside the vacuum chamber. A  $^{22}\text{Na}$  radioisotope of 220 kBq is used as the positron source. The emitted positrons are tagged by a 0.2-mm-thick plastic scintillator. The scintillation light is detected by the fine-mesh PMT and the signals are used to obtain the timing information of Ps formation.

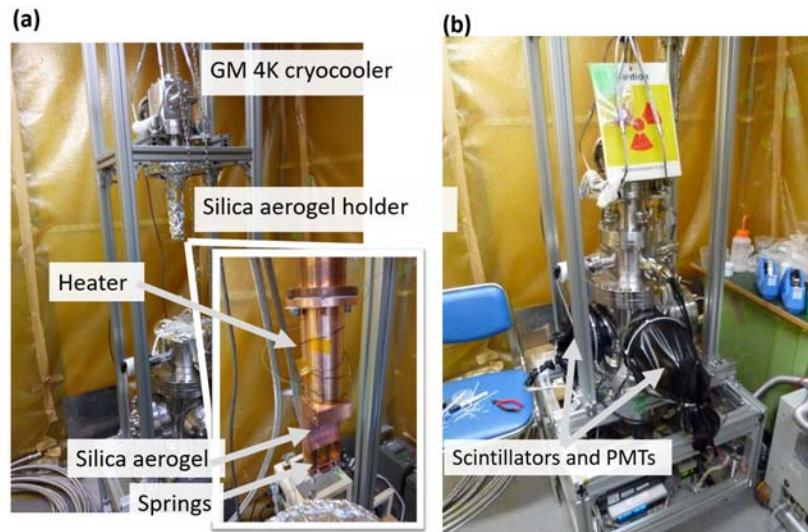


**Fig. 7** Photographs of the experimental setup of the Ps thermalization measurement. (a) Inside the vacuum chamber. The magnified view of the target and the cold stage is inserted. (b) Outside the vacuum chamber.

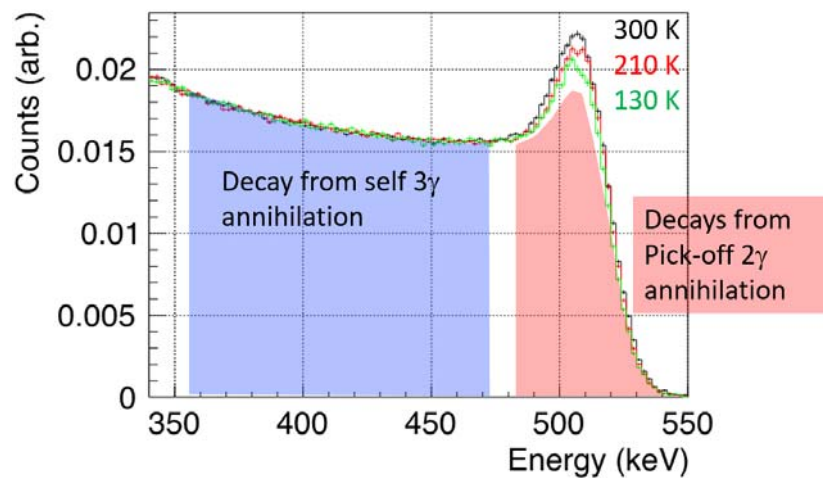


**Fig. 8** Energy spectra of annihilation gamma-rays at 30 ns–600 ns from Ps formation. Data at 300 K, 210 K, and 130 K are shown by different lines. Shaded regions show the self 3 $\gamma$  and pick-off 2 $\gamma$  annihilation-dominant regions.

A porous silica aerogel target is used as the Ps converter. The target density is  $0.11 \text{ g cm}^{-3}$ , which corresponds to a Ps mean free path of 38 nm assuming the silica particle diameter to be 3.0 nm. The target is attached to a cold stage by springs to ensure thermal coupling. The temperature of the target is controlled between 20 K and 300 K using a GM 4-K cryocooler and a heater. The temperatures of the cold stage and the silica target are monitored by Si sensors. The target is cut into 2 pieces and the Si sensor is sandwiched in between. A  $\text{LaBr}_3(\text{Ce})$  scintillator and the fine-mesh PMT are used to measure the timing and energy of  $\gamma$ -rays from Ps decay. The signals are collected and processed using NIM and CAMAC systems.

The vacuum chamber is kept pumped by a turbo pump during the measurement. The base pressure



is  $10^{-5}$  Pa. The measurements are performed at target temperatures of 300 K, 210 K, 130 K, and 20 K. Each measurement takes  $\sim 1$  week. The data are analyzed using Monte Carlo simulations generated by Geant4 [20,21]. The geometry and materials of the setup are input carefully to the simulation.

### 3.4 Preliminary results

As preliminary results, the 300 K, 210 K, and 130 K data are presented here. The 20 K data are currently under careful analysis.

Figure 8 shows the energy spectra of annihilation  $\gamma$ -rays with elapsed times over 30 ns–600 ns from Ps formation. Accidental spectra are already subtracted using energy spectra at 1200 ns–1500 ns. The  $3\gamma$  self-annihilations and the pick-off  $2\gamma$  annihilations can be separated by the energy information. All the spectra are normalized by the area of the  $3\gamma$ -self-annihilation-dominant region, since the  $3\gamma$  annihilation rate  $\lambda_3 = 7.04 \mu\text{s}^{-1}$  does not depend on the Ps temperature. Less pick-off  $2\gamma$  annihilations are seen by cooling Ps to lower temperature.

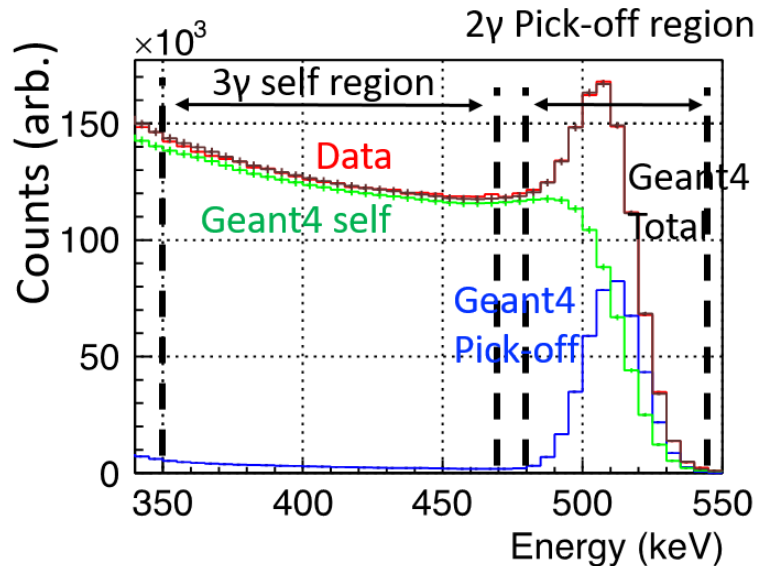


**Fig. 9** Typical fitting of energy spectrum by Monte Carlo simulation. The data at 30 ns–600 ns from Ps formation is shown. Accidental spectrum is already subtracted.

Figure 9 shows a typical fitting of the energy spectrum by a Monte Carlo simulation. The fitting is performed using the data in the  $3\gamma$  self-annihilation region and the  $2\gamma$  pick-off region. The Monte Carlo simulation can explain the data well. The ratio of the two different annihilations  $\lambda_2/\lambda_3$  is obtained by this fitting result.

Figure 10 shows the time evolution of  $\lambda_2/\lambda_3$  at various temperatures. The data are fitted by Eq. (1) using  $\lambda_2(t) = Cv(t)/L$ , where  $C$  is a constant. The conversion from  $\lambda_2/\lambda_3$  to Ps temperature shown on the right-hand vertical axis has been performed under the naive assumption that  $\lambda_2$  is proportional to  $n\sigma v$ . Ps thermalization into  $\sim 130$  K is clearly observed. The fitting result is  $M = 255(17)u$  (hereafter, the value in the parentheses, following each number, denotes the standard deviation), where  $u$  is the unified atomic mass unit, with the Ps initial kinetic energy  $E_0 = 0.158(0.008)$  eV ( $\chi^2/\text{ndf} = 46.6/27$ ,  $p$ -value = 0.011). These numbers are preliminary since we have not yet checked whether the naive assumption used in the fitting can be also used for the 20 K data. A careful and self-consistent analysis including the 20 K data is ongoing, results of which will finally determine the thermalization

parameters necessary for study of Ps-BEC. Fig. 3 is plotted using the preliminary numbers. These values are shown to be small enough to realize Ps-BEC under our assumption. This conclusion will be finally checked by completion of the thermalization analysis.

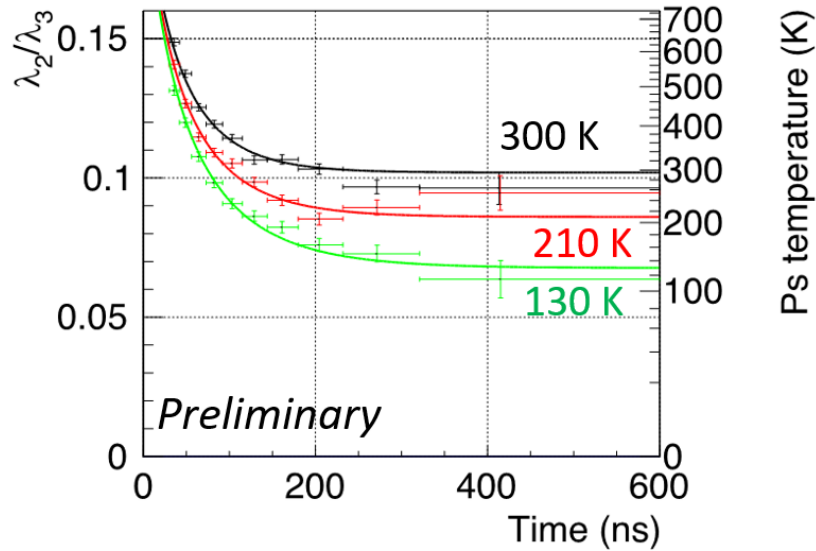


**Fig. 10** Time evolution of pick-off ratio at 300 K, 210 K, and 130 K. The points with error bars are the data, and the solid lines are the fitting result.

## 4. Positronium cooling laser

### 4.1 Design

The second stage of Ps cooling of our method for Ps-BEC is performed by laser cooling. The laser wavelength is 243 nm to stimulate 1S-2P transitions. The following special features are necessary for Ps laser cooling.

*Long pulse width:* As shown in Fig. 3, the cooling of Ps takes around 350 ns to realize Ps-BEC. A pulse width of 300 ns at  $2\sigma$  is required.

*Wide linewidth:* The Doppler effect of Ps is large due to the light Ps mass, so the laser linewidth must cover the wide Doppler width.

*Fast shift of wavelength:* The resonant wavelength shifts as Ps atoms get cold. The laser wavelength should also be shifted according to the cooling. This fast shift (40 pm in 300 ns) of pulsed laser

**Table I** Ps cooling laser requirements.

Parameter	Required value
Wavelength	243 nm
Pulse energy	40 $\mu$ J
Pulse width	300 ns
Linewidth	80 pm
Wavelength shift	40 pm in 300 ns
Beam size	200 $\mu$ m



has never been achieved anywhere.

The requirements are summarized in Table I. To satisfy these special requirements, we proposed a new design of the laser system in Refs. 13 and 14.

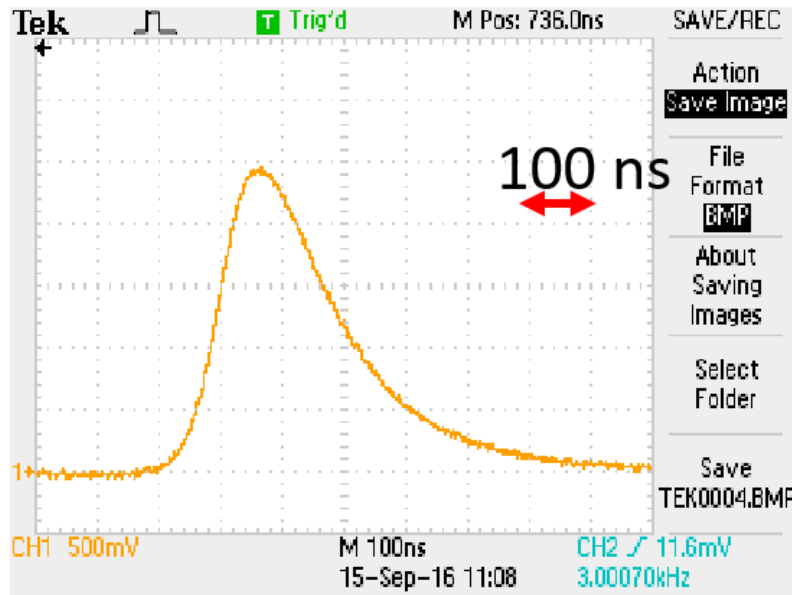


**Fig. 11** 729 nm pulse from the prototype Ti:Sapphire cavity detected by a photodiode. The vertical scale is arbitrary.

## 4.2 Status of laser development

A new laser system is under development based on our new design. A seed CW laser of 729 nm wavelength has been developed using an external-cavity diode laser (ECDL). A prototype bow-tie cavity with a Ti:Sapphire crystal has also been constructed. Using a low-power Nd:YAG pulsed pump laser (532 nm) and injection locking with the seed laser, we have obtained 200-ns-long pulses at 729 nm (Fig. 11). We have also succeeded in generating 365 nm pulses using an LBO crystal.

## 5. Summary

Ps-BEC is expected to be the first BEC of any system which contains an antiparticle. It can be a powerful probe for fundamental physics. It can also be used to realize a  $\gamma$ -ray laser. A new method to realize Ps-BEC was proposed and a basic study to focus positron beams to 100 nm waist has been started. To estimate the effect of the first-stage of Ps cooling by thermalization, the Ps thermalization process in cryogenic environment was observed for the first time. The preliminary results suggest that Ps can be cooled quickly enough for the formation of a Ps-BEC. The second-stage of Ps cooling will be performed by Ps laser cooling. A new 243 nm laser system was designed and is currently under development. The next step is to perform the first laser cooling of Ps, which is also the first laser cooling of any system which contains an antiparticle. In parallel with the development of a dense positron beam, the productions of a Ps-BEC will be targeted.

## References

- [1] A. Ishida, T. Namba, S. Asai, T. Kobayashi, H. Saito, M. Yoshida, K. Tanaka, and A. Yamamoto, Phys.

- Lett. B **734**, 338 (2014).
- [2] A. Miyazaki, T. Yamazaki, T. Suehara, T. Namba, S. Asai, T. Kobayashi, H. Saito, Y. Tatematsu, I. Ogawa, and T. Idehara, Prog. Theor. Exp. Phys. **2015**, 011C01 (2015).
  - [3] Y. Kataoka, S. Asai, and T. Kobayashi, Phys. Lett. B **671**, 219 (2009).
  - [4] A. H. Al-Ramadhan and G. W. Gidley, Phys. Rev. Lett. **72**, 1632 (1994).
  - [5] M. S. Fee, A. P. Mills, Jr., S. Chu, E. D. Shaw, K. Danzmann, R. J. Chichester, and D. M. Zuckerman, Phys. Rev. Lett. **70**, 1397 (1993).
  - [6] T. Yamazaki, T. Namba, S. Asai, and T. Kobayashi, Phys. Rev. Lett. **104**, 083401 (2010).
  - [7] P. A. Vetter and S. J. Freedman, Phys. Rev. Lett. **91**, 263401 (2003).
  - [8] S. G. Karshenboim, Astr. Lett. **35**, 663 (2009).
  - [9] D. B. Cassidy and A. P. Mills, Jr., phys. stat. sol. (c) **4**, 3419 (2007).
  - [10] C. B. Stevens, EIR Science & Technology **13**(43), 22 (1986).
  - [11] H. K. Avetissian, A. K. Avetissian, and G. F. Mkrtchian, Phys. Rev. Lett. **113**, 023904 (2014).
  - [12] H. K. Avetissian, A. K. Avetissian, and G. F. Mkrtchian, Phys. Rev. A **92**, 023820 (2015).
  - [13] K. Shu, X. Fan, T. Yamazaki, T. Namba, S. Asai, K. Yoshioka, and M. Kuwata-Gonokami, J. Phys. B: At. Mol. Opt. Phys. **49**, 104001 (2016).
  - [14] K. Shu, T. Murayoshi, X. Fan, A. Ishida, T. Yamazaki, T. Namba, S. Asai, K. Yoshioka, M. Kuwata-Gonokami, N. Oshima, B. E. O'Rourke, and R. Suzuki, J. Phys.: Conf. Ser. **791**, 012007 (2017).
  - [15] N. Oshima, R. Suzuki, T. Ohdaira, A. Kinomura, T. Narumi, A. Uedono, and M. Fujinami, J. Appl. Phys. **103**, 094916 (2008).
  - [16] Y. Nagashima, M. Kakimoto, T. Hyodo, K. Fujiwara, A. Ichimura, T. Chang, J. Deng, T. Akahane, T. Chiba, K. Suzuki, B. T. A. McKee, and A. T. Stewart, Phys. Rev. A **52**, 258 (1995).
  - [17] T. Chang, M. Xu, and X. Zeng, Phys. Lett. A **126**, 189 (1987).
  - [18] K. Shibuya, Y. Kawamura, and H. Saito, Phys. Rev. A **88**, 042517 (2013).
  - [19] Y. Nagashima, T. Hyodo, K. Fujiwara, and A. Ichimura, J. Phys. B: At. Mol. Opt. Phys. **31**, 329 (1998).
  - [20] S. Agostinelli et al., Nucl. Instr. and Meth. Phys. Res. A **506**, 250 (2003).
  - [21] J. Allison et al., IEEE Trans. Nucl. Sci. **53**, 270 (2006).